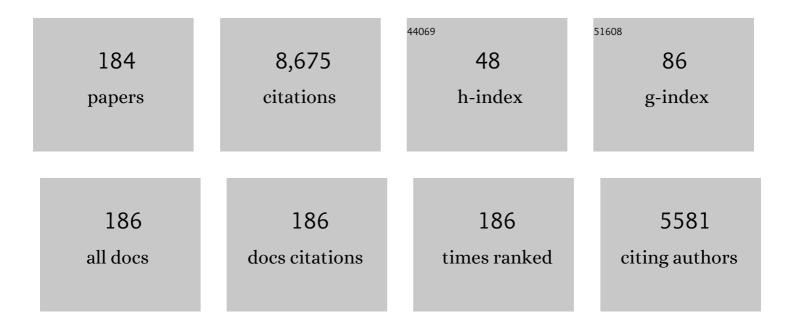
Shucheng Xie

List of Publications by Year in descending order

Source: https://exaly.com/author-pdf/5154432/publications.pdf Version: 2024-02-01



#	Article	IF	CITATIONS
1	Quantification of Holocene Asian monsoon rainfall from spatially separated cave records. Earth and Planetary Science Letters, 2008, 266, 221-232.	4.4	626
2	Two episodes of microbial change coupled with Permo/Triassic faunal mass extinction. Nature, 2005, 434, 494-497.	27.8	297
3	Rapid oxygenation of Earth's atmosphere 2.33 billion years ago. Science Advances, 2016, 2, e1600134.	10.3	264
4	n-Alkane distributions in ombrotrophic mires as indicators of vegetation change related to climatic variation. Organic Geochemistry, 2000, 31, 231-235.	1.8	250
5	Changes in the global carbon cycle occurred as two episodes during the Permian–Triassic crisis. Geology, 2007, 35, 1083.	4.4	246
6	A highly redox-heterogeneous ocean in South China during the early Cambrian (â^¼529–514ÂMa): Implications for biota-environment co-evolution. Earth and Planetary Science Letters, 2016, 441, 38-51.	4.4	198
7	Molecular and isotopic stratigraphy in an ombrotrophic mire for paleoclimate reconstruction. Geochimica Et Cosmochimica Acta, 2004, 68, 2849-2862.	3.9	190
8	East Asian hydroclimate modulated by the position of the westerlies during Termination I. Science, 2018, 362, 580-583.	12.6	190
9	Reconstruction of late glacial and Holocene climate evolution in southern China from geolipids and pollen in the Dingnan peat sequence. Organic Geochemistry, 2005, 36, 1272-1284.	1.8	189
10	Lipid biomarkers in the Zoigê-Hongyuan peat deposit: Indicators of Holocene climate changes in West China. Organic Geochemistry, 2007, 38, 1927-1940.	1.8	183
11	Concordant monsoon-driven postglacial hydrological changes in peat and stalagmite records and their impacts on prehistoric cultures in central China. Geology, 2013, 41, 827-830.	4.4	169
12	Correlations between microbial tetraether lipids and environmental variables in Chinese soils: Optimizing the paleo-reconstructions in semi-arid and arid regions. Geochimica Et Cosmochimica Acta, 2014, 126, 49-69.	3.9	160
13	Changes in marine productivity and redox conditions during the Late Ordovician Hirnantian glaciation. Palaeogeography, Palaeoclimatology, Palaeoecology, 2015, 420, 223-234.	2.3	157
14	Cyanobacterial blooms tied to volcanism during the 5 m.y. Permo-Triassic biotic crisis. Geology, 2010, 38, 447-450.	4.4	151
15	Holocene ENSO-related cyclic storms recorded by magnetic minerals in speleothems of central China. Proceedings of the National Academy of Sciences of the United States of America, 2017, 114, 852-857.	7.1	149
16	Links between the East Asian monsoon and North Atlantic climate during the 8,200 year event. Nature Geoscience, 2013, 6, 117-120.	12.9	147
17	lsotopic evidence for an anomalously low oceanic sulfate concentration following end-Permian mass extinction. Earth and Planetary Science Letters, 2010, 300, 101-111.	4.4	145
18	Postglacial climate-change record in biomarker lipid compositions of the Hani peat sequence, Northeastern China. Earth and Planetary Science Letters, 2010, 294, 37-46.	4.4	138

#	Article	IF	CITATIONS
19	The 6-methyl branched tetraethers significantly affect the performance of the methylation index (MBT′) in soils from an altitudinal transect at Mount Shennongjia. Organic Geochemistry, 2015, 82, 42-53.	1.8	134
20	Evidence of moisture control on the methylation of branched glycerol dialkyl glycerol tetraethers in semi-arid and arid soils. Geochimica Et Cosmochimica Acta, 2016, 189, 24-36.	3.9	110
21	Microbial lipid records of highly alkaline deposits and enhanced aridity associated with significant uplift of the Tibetan Plateau in the Late Miocene. Geology, 2012, 40, 291-294.	4.4	106
22	Negative C-isotope excursions at the Permian-Triassic boundary linked to volcanism. Geology, 2012, 40, 963-966.	4.4	101
23	Reduction of structural Fe(III) in nontronite by methanogen Methanosarcina barkeri. Geochimica Et Cosmochimica Acta, 2011, 75, 1057-1071.	3.9	96
24	Uncovering the spatial heterogeneity of Ediacaran carbon cycling. Geobiology, 2017, 15, 211-224.	2.4	91
25	Comparative microbial diversity and redox environments of black shale and stromatolite facies in the Mesoproterozoic Xiamaling Formation. Geochimica Et Cosmochimica Acta, 2015, 151, 150-167.	3.9	89
26	Mercury evidence of intense volcanic effects on land during the Permian-Triassic transition. Geology, 2019, 47, 1117-1121.	4.4	89
27	Enhanced nitrogen fixation in the immediate aftermath of the latest Permian marine mass extinction. Geology, 2011, 39, 647-650.	4.4	88
28	The potential of biomarker proxies to trace climate, vegetation, and biogeochemical processes in peat: A review. Global and Planetary Change, 2019, 179, 57-79.	3.5	82
29	Lipid distribution in a subtropical southern China stalagmite as a record of soil ecosystem response to paleoclimate change. Quaternary Research, 2003, 60, 340-347.	1.7	81
30	Different temperature dependence of the bacterial brGDGT isomers in 35 Chinese lake sediments compared to that in soils. Organic Geochemistry, 2018, 119, 72-79.	1.8	81
31	Two episodes of environmental change at the Permian–Triassic boundary of the CSSP section Meishan. Earth-Science Reviews, 2012, 115, 163-172.	9.1	79
32	Massive formation of early diagenetic dolomite in the Ediacaran ocean: Constraints on the "dolomite problem― Proceedings of the National Academy of Sciences of the United States of America, 2020, 117, 14005-14014.	7.1	78
33	An interlaboratory study of TEX ₈₆ and BIT analysis of sediments, extracts, and standard mixtures. Geochemistry, Geophysics, Geosystems, 2013, 14, 5263-5285.	2.5	76
34	U/Mo ratios and Î'98/95Mo as local and global redox proxies during mass extinction events. Chemical Geology, 2012, 324-325, 99-107.	3.3	68
35	A 13,000-year peatland palaeohydrological response to the ENSO-related Asian monsoon precipitation changes in the middle Yangtze Valley. Quaternary Science Reviews, 2019, 212, 80-91.	3.0	68
36	Shallow stratification prevailed for â^1⁄41700 to â^1⁄41300 Ma ocean: Evidence from organic carbon isotopes in the North China Craton. Earth and Planetary Science Letters, 2014, 400, 219-232.	4.4	66

#	Article	IF	CITATIONS
37	Lipid distributions in loess-paleosol sequences from northwest China. Organic Geochemistry, 2003, 34, 1071-1079.	1.8	65
38	Decline in oceanic sulfate levels during the early Mesoproterozoic. Precambrian Research, 2015, 258, 36-47.	2.7	65
39	Response of carbon cycle to drier conditions in the mid-Holocene in central China. Nature Communications, 2018, 9, 1369.	12.8	60
40	Ediacaran Marine Redox Heterogeneity and Early Animal Ecosystems. Scientific Reports, 2015, 5, 17097.	3.3	59
41	Stepwise and large-magnitude negative shift in δ13Ccarb preceded the main marine mass extinction of the Permian–Triassic crisis interval. Palaeogeography, Palaeoclimatology, Palaeoecology, 2011, 299, 70-82.	2.3	58
42	Paleotemperature variability in central China during the last 13 ka recorded by a novel microbial lipid proxy in the Dajiuhu peat deposit. Holocene, 2013, 23, 1123-1129.	1.7	58
43	A theoretical prediction of chemical zonation in early oceans (>520 Ma). Science China Earth Sciences, 2015, 58, 1901-1909.	5.2	58
44	Paleo-seawater REE compositions and microbial signatures preserved in laminae of Lower Triassic ooids. Palaeogeography, Palaeoclimatology, Palaeoecology, 2017, 486, 96-107.	2.3	58
45	Mercury fluxes record regional volcanism in the South China craton prior to the end-Permian mass extinction. Geology, 2021, 49, 452-456.	4.4	57
46	Vertical δ13Corg gradients record changes in planktonic microbial community composition during the end-Permian mass extinction. Palaeogeography, Palaeoclimatology, Palaeoecology, 2014, 396, 119-131.	2.3	52
47	Occurrence of tetraether lipids in stalagmites: Implications for sources and GDGT-based proxies. Organic Geochemistry, 2011, 42, 108-115.	1.8	50
48	Nitrogen fixation sustained productivity in the wake of the Palaeoproterozoic Great Oxygenation Event. Nature Communications, 2018, 9, 978.	12.8	50
49	Size variation of conodont elements of the Hindeodus–Isarcicella clade during the Permian–Triassic transition in South China and its implication for mass extinction. Palaeogeography, Palaeoecology, 2008, 264, 176-187.	2.3	49
50	Microbial–algal community changes during the latest Permian ecological crisis: Evidence from lipid biomarkers at Cili, South China. Global and Planetary Change, 2013, 105, 36-51.	3.5	49
51	Intensified continental chemical weathering and carbon-cycle perturbations linked to volcanism during the Triassic–Jurassic transition. Nature Communications, 2022, 13, 299.	12.8	49
52	Hydroxylated isoprenoid GDGTs in Chinese coastal seas and their potential as a paleotemperature proxy for mid-to-low latitude marginal seas. Organic Geochemistry, 2015, 89-90, 31-43.	1.8	48
53	Contrasting microbial community changes during mass extinctions at the Middle/Late Permian and Permian/Triassic boundaries. Earth and Planetary Science Letters, 2017, 460, 180-191.	4.4	48
54	Comparison of free lipid compositions between roots and leaves of plants in the Dajiuhu Peatland, central China. Geochemical Journal, 2011, 45, 365-373.	1.0	47

#	Article	IF	CITATIONS
55	Soil pH impact on microbial tetraether lipids and terrestrial input index (BIT) in China. Science China Earth Sciences, 2012, 55, 236-245.	5.2	46
56	Paleoclimate influence on early diagenesis of plant triterpenes in the Dajiuhu peatland, central China. Geochimica Et Cosmochimica Acta, 2013, 123, 106-119.	3.9	46
57	The occurrence of a grassy vegetation over the Chinese Loess Plateau since the last interglacier: the molecular fossil record. Science in China Series D: Earth Sciences, 2002, 45, 53-62.	0.9	45
58	Distribution of glycerol dialkyl glycerol tetraether (GDGT) lipids in a hypersaline lake system. Organic Geochemistry, 2016, 99, 113-124.	1.8	45
59	Microbial glycerol dialkyl glycerol tetraethers from river water and soil near the Three Gorges Dam on the Yangtze River. Organic Geochemistry, 2013, 56, 40-50.	1.8	44
60	Perturbation of the marine nitrogen cycle during the Late Ordovician glaciation and mass extinction. Palaeogeography, Palaeoclimatology, Palaeoecology, 2016, 448, 339-348.	2.3	44
61	Environmental impacts on the distribution of microbial tetraether lipids in Chinese lakes with contrasting pH: Implications for lacustrine paleoenvironmental reconstructions. Science China Earth Sciences, 2016, 59, 939-950.	5.2	42
62	Distribution of aliphatic des-A-triterpenoids in the Dajiuhu peat deposit, southern China. Organic Geochemistry, 2008, 39, 1765-1771.	1.8	41
63	Molecular records of microbialites following the end-Permian mass extinction in Chongyang, Hubei Province, South China. Palaeogeography, Palaeoclimatology, Palaeoecology, 2011, 308, 151-159.	2.3	41
64	Occurrence of diploptene in moss species from the Dajiuhu Peatland in southern China. Organic Geochemistry, 2010, 41, 321-324.	1.8	40
65	Sources and distribution of isoprenoid glycerol dialkyl glycerol tetraethers (GDGTs) in sediments from the east coastal sea of China: Application of GDGT-based paleothermometry to a shallow marginal sea. Organic Geochemistry, 2014, 75, 24-35.	1.8	40
66	Variations in dissolved O2 in a Chinese lake drive changes in microbial communities and impact sedimentary GDGT distributions. Chemical Geology, 2021, 579, 120348.	3.3	40
67	Lipid biomarkers for the reconstruction of deep-time environmental conditions. Earth-Science Reviews, 2019, 189, 99-124.	9.1	39
68	Rapid response of fossil tetraether lipids in lake sediments to seasonal environmental variables in a shallow lake in central China: Implications for the use of tetraether-based proxies. Organic Geochemistry, 2019, 128, 108-121.	1.8	38
69	Absence of a significant bias towards summer temperature in branched tetraether-based paleothermometer at two soil sites with contrasting temperature seasonality. Organic Geochemistry, 2016, 94, 83-94.	1.8	37
70	Molecular fossils in a Pleistocene river terrace in southern China related to paleoclimate variation. Organic Geochemistry, 2003, 34, 789-797.	1.8	36
71	Antarctic link with East Asian summer monsoon variability during the Heinrich Stadial–BÃ,lling interstadial transition. Earth and Planetary Science Letters, 2016, 453, 243-251.	4.4	36
72	Restricted utility of δ13C of bulk organic matter as a record of paleovegetation in some loess–Paleosol sequences in the Chinese Loess Plateau. Quaternary Research, 2004, 62, 86-93.	1.7	35

#	Article	IF	CITATIONS
73	Leaf wax n-alkane chemotaxonomy of bamboo from a tropical rain forest in Southwest China. Plant Systematics and Evolution, 2012, 298, 731-738.	0.9	35
74	Spatiotemporal variability of ocean chemistry in the early Cambrian, South China. Science China Earth Sciences, 2014, 57, 579-591.	5.2	35
75	Geochemical analyses of a Himalayan snowpit profile: implications for atmospheric pollution and climate. Organic Geochemistry, 2000, 31, 15-23.	1.8	34
76	Significance of long chain iso and anteiso monomethyl alkanes in the Lamiaceae (mint family). Organic Geochemistry, 2011, 42, 156-165.	1.8	34
77	Distributions of isoprenoid and branched glycerol dialkanol diethers in Chinese surface soils and a loess–paleosol sequence: Implications for the degradation of tetraether lipids. Organic Geochemistry, 2014, 66, 70-79.	1.8	32
78	5-n-Alkylresorcinols as biomarkers of sedges in an ombrotrophic peat section. Organic Geochemistry, 2002, 33, 861-867.	1.8	31
79	Adsorbed silica in stalagmite carbonate and its relationship to past rainfall. Geochimica Et Cosmochimica Acta, 2005, 69, 2285-2292.	3.9	31
80	Impacts of pH and temperature on soil bacterial 3-hydroxy fatty acids: Development of novel terrestrial proxies. Organic Geochemistry, 2016, 94, 21-31.	1.8	30
81	Diversity, distribution and biogeography of testate amoebae in China: Implications for ecological studies in Asia. European Journal of Protistology, 2011, 47, 1-9.	1.5	29
82	Environmental factors affecting the low temperature isomerization of homohopanes in acidic peat deposits, central China. Geochimica Et Cosmochimica Acta, 2015, 154, 212-228.	3.9	29
83	Tropical and high latitude forcing of enhanced megadroughts in Northern China during the last four terminations. Earth and Planetary Science Letters, 2017, 479, 98-107.	4.4	29
84	Characterstics of seasonal variations of leaf n-alkanes and n-alkenes in modern higher plants in Qingjiang, Hubei Province, China. Science Bulletin, 2008, 53, 2659-2664.	9.0	28
85	A 9000-year carbon isotopic record of acid-soluble organic matter in a stalagmite from Heshang Cave, central China: Paleoclimate implications. Chemical Geology, 2014, 388, 71-77.	3.3	28
86	Holocene temperature and hydrological changes reconstructed by bacterial 3-hydroxy fatty acids in a stalagmite from central China. Quaternary Science Reviews, 2018, 192, 97-105.	3.0	28
87	Distribution of pyrolytic PAHs across the Triassic-Jurassic boundary in the Sichuan Basin, southwestern China: Evidence of wildfire outside the Central Atlantic Magmatic Province. Earth-Science Reviews, 2020, 201, 102970.	9.1	27
88	Phytoliths and microcharcoal at Jinluojia archeological site in middle reaches of Yangtze River indicative of paleoclimate and human activity during the last 3000 years. Journal of Archaeological Science, 2010, 37, 124-132.	2.4	26
89	Moisture conditions during the Younger Dryas and the early Holocene in the middle reaches of the Yangtze River, central China. Holocene, 2012, 22, 1473-1479.	1.7	26
90	The Pleistocene vermicular red earth in South China signaling the global climatic change: The molecular fossil record. Science in China Series D: Earth Sciences, 2003, 46, 1113-1120.	0.9	25

#	Article	IF	CITATIONS
91	Testate amoebae as indicators of 20th century environmental change in Lake Zhangdu, China. Fundamental and Applied Limnology, 2009, 175, 29-38.	0.7	25
92	Expansion of photic-zone euxinia during the Permian–Triassic biotic crisis and its causes: Microbial biomarker records. Palaeogeography, Palaeoclimatology, Palaeoecology, 2017, 474, 140-151.	2.3	25
93	Multiple sulfur-isotopic evidence for a shallowly stratified ocean following the Triassic-Jurassic boundary mass extinction. Geochimica Et Cosmochimica Acta, 2018, 231, 73-87.	3.9	25
94	Biomarker evidence of algal-microbial community changes linked to redox and salinity variation, Upper Devonian Chattanooga Shale (Tennessee, USA). Bulletin of the Geological Society of America, 2021, 133, 409-424.	3.3	25
95	The fluctuating environment associated with the episodic biotic crisis during the Permo/Triassic transition: Evidence from microbial biomarkers in Changxing, Zhejiang Province. Science in China Series D: Earth Sciences, 2007, 50, 1052-1059.	0.9	22
96	The prelude of the end-Permian mass extinction predates a postulated bolide impact. International Journal of Earth Sciences, 2007, 96, 903-909.	1.8	20
97	A comparative study of n-alkane biomarker and pollen records: an example from southern China. Science Bulletin, 2009, 54, 1065-1072.	9.0	20
98	Optimization of acid digestion conditions on the extraction of fatty acids from stalagmites. Frontiers of Earth Science, 2012, 6, 109-114.	2.1	20
99	Variations in wetland hydrology drive rapid changes in the microbial community, carbon metabolic activity, and greenhouse gas fluxes. Geochimica Et Cosmochimica Acta, 2022, 317, 269-285.	3.9	20
100	Distributions of fatty acids in a stalagmite related to paleoclimate change at Qingjiang in Hubei, southern China. Science in China Series D: Earth Sciences, 2005, 48, 1463.	0.9	19
101	The Response of Archaeal Tetraether Membrane Lipids in Surface Soils to Temperature: A Potential Paleothermometer in Paleosols. Geomicrobiology Journal, 2016, 33, 98-109.	2.0	19
102	Assessing hydroxylated isoprenoid GDGTs as a paleothermometer for the tropical South China Sea. Organic Geochemistry, 2018, 115, 156-165.	1.8	19
103	Chemotaxonomic significance of n-alkane distributions from leaf wax in genus of Sinojackia species (Styracaceae). Biochemical Systematics and Ecology, 2013, 49, 30-36.	1.3	18
104	Spurious thermoluminescence characteristics of the Ediacaran Doushantuo Formation (ca. 635–551) Tj ETQq((Wuhan, China), 2015, 26, 883-892.) 0 0 rgBT 3.2	/Overlock 10 18
105	Coupled oceanic oxygenation and metazoan diversification during the early–middle Cambrian?. Geology, 0, , G39208.1.	4.4	18
106	Asian monsoon evolution linked to Pacific temperature gradients since the Late Miocene. Earth and Planetary Science Letters, 2021, 563, 116882.	4.4	18
107	Reconstructing late Holocene palaeoenvironments in Bangladesh: phytolith analysis of archaeological soils from Somapura Mahavihara site in the Paharpur area, Badalgacchi Upazila, Naogaon District, Bangladesh. Journal of Archaeological Science, 2009, 36, 504-512.	2.4	17
108	Seasonal variation of fatty acids from drip water in Heshang Cave, central China. Applied Geochemistry, 2011, 26, 341-347.	3.0	17

#	Article	IF	CITATIONS
109	Distribution of branched tetraether lipids in ponds from Inner Mongolia, NE China: Insight into the source of brGDGTs. Organic Geochemistry, 2017, 112, 127-136.	1.8	17
110	The elemental enrichments at Dajiuhu Peatland in the Middle Yangtze Valley in response to changes in East Asian monsoon and human activity since 20,000ÂcalÂyr BP. Science of the Total Environment, 2021, 757, 143990.	8.0	17
111	Progress and perspective on frontiers of geobiology. Science China Earth Sciences, 2014, 57, 855-868.	5.2	16
112	Mo marine geochemistry and reconstruction of ancient ocean redox states. Science China Earth Sciences, 2015, 58, 2123-2133.	5.2	16
113	Paleoaltimetry proxies based on bacterial branched tetraether membrane lipids in soils. Frontiers of Earth Science, 2015, 9, 13-25.	2.1	16
114	Developing a continental-scale testate amoeba hydrological transfer function for Asian peatlands. Quaternary Science Reviews, 2021, 258, 106868.	3.0	16
115	Microbial and molecular fossils from the Permian Zoophycos in South China. Science in China Series D: Earth Sciences, 2007, 50, 1121-1127.	0.9	15
116	Volcanism in Association with the Prelude to Mass Extinction and Environment Change Across the Permian-Triassic Boundary (PTB), Southern China. Clays and Clay Minerals, 2011, 59, 478-489.	1.3	15
117	Paleofire indicated by polycyclic aromatic hydrocarbons in soil of Jinluojia archaeological site, Hubei, China. Journal of Earth Science (Wuhan, China), 2010, 21, 247-256.	3.2	14
118	Glomalinâ€related soil protein distributions in the wetlands of the Liaohe Delta, Northeast China: Implications for carbon sequestration and mineral weathering of coastal wetlands. Limnology and Oceanography, 2020, 65, 979-991.	3.1	14
119	Variation of branched tetraethers with soil depth in relation to non-temperature factors: Implications for paleoclimate reconstruction. Chemical Geology, 2021, 572, 120211.	3.3	14
120	Clay mineralogy of archaeological soil: an approach to paleoclimatic and environmental reconstruction of the archaeological sites of the Paharpur area, Badalgacchi upazila, Naogaon district, Bangladesh. Environmental Geology, 2008, 53, 1639-1650.	1.2	13
121	Magnetic fabric of stalagmites and its formation mechanism. Geochemistry, Geophysics, Geosystems, 2012, 13, .	2.5	13
122	Distribution of microbial lipids at an acid mine drainage site in China: Insights into microbial adaptation to extremely low pH conditions. Organic Geochemistry, 2019, 134, 77-91.	1.8	13
123	A new sea surface temperature proxy based on bacterial 3-hydroxy fatty acids. Organic Geochemistry, 2020, 141, 103975.	1.8	13
124	On the geobiological evaluation of hydrocarbon source rocks. Frontiers of Earth Science, 2007, 1, 389-398.	0.5	12
125	Archaeal and bacterial tetraether membrane lipids in soils of varied altitudes in Mt. Jianfengling in South China. Journal of Earth Science (Wuhan, China), 2010, 21, 277-280.	3.2	12
126	Relationships between carbon isotope evolution and variation of microbes during the Permian–Triassic transition at Meishan Section, South China. International Journal of Earth Sciences, 2010, 99, 775-784.	1.8	12

#	Article	IF	CITATIONS
127	Distinct distribution revealing multiple bacterial sources for 1-O-monoalkyl glycerol ethers in terrestrial and lake environments. Science China Earth Sciences, 2015, 58, 1005-1017.	5.2	12
128	Testate amoebae as indicators of water quality and contamination in shallow lakes of the Middle and Lower Yangtze Plain. Environmental Earth Sciences, 2016, 75, 1.	2.7	12
129	The Early Pliocene global expansion of C4 grasslands: A new organic carbon-isotopic dataset from the north China plain. Palaeogeography, Palaeoclimatology, Palaeoecology, 2020, 538, 109454.	2.3	12
130	Holocene peatland water regulation response to ~1000-year solar cycle indicated by phytoliths in central China. Journal of Hydrology, 2020, 589, 125169.	5.4	12
131	Discussion on geobiology, biogeology and geobiofacies. Science in China Series D: Earth Sciences, 2008, 51, 1516-1524.	0.9	11
132	n-alkanol ratios as proxies of paleovegetation and paleoclimate in a peat-lacustrine core in southern China since the last deglaciation. Frontiers of Earth Science, 2009, 3, 445-451.	0.5	11
133	Geomicrobial functional groups: A window on the interaction between life and environments. Science Bulletin, 2012, 57, 2-19.	1.7	11
134	Distribution of microbial fatty acids and fatty alcohols in soils from an altitude transect of Mt. Jianfengling in Hainan, China: Implication for paleoaltimetry and paleotemperature reconstruction. Science China Earth Sciences, 2014, 57, 999-1012.	5.2	11
135	Global calibration of novel 3-hydroxy fatty acid based temperature and pH proxies. Geochimica Et Cosmochimica Acta, 2021, 302, 101-119.	3.9	11
136	Distribution and Geochemical Implication of Aromatic Hydrocarbons across the Meishan Permian-Triassic Boundary. Journal of China University of Geosciences, 2006, 17, 49-54.	0.5	10
137	Flooding impact on the distribution of microbial tetraether lipids in paddy rice soil in China. Frontiers of Earth Science, 2013, 7, 384-394.	2.1	10
138	Distribution of archaeal and bacterial tetraether membrane lipids in rhizosphere-root systems in soils and their implication for paleoclimate assessment. Geochemical Journal, 2013, 47, 337-347.	1.0	10
139	Changes in vegetation type on the Chinese Loess Plateau since 75â€ [−] ka related to East Asian Summer Monsoon variation. Palaeogeography, Palaeoclimatology, Palaeoecology, 2018, 510, 124-139.	2.3	10
140	Land-use change effects on protozoic silicon pools in the Dajiuhu National Wetland Park, China. Geoderma, 2020, 368, 114305.	5.1	10
141	Multiple environmental and ecological controls on archaeal ether lipid distributions in saline ponds. Chemical Geology, 2019, 529, 119293.	3.3	9
142	Intensified Ocean Deoxygenation During the end Devonian Mass Extinction. Geochemistry, Geophysics, Geosystems, 2019, 20, 6187-6198.	2.5	9
143	Pentagonia zhangduensis nov. spec. (Lobosea, Arcellinida), a new freshwater species from China. European Journal of Protistology, 2008, 44, 287-290.	1.5	8
144	Occurrence of highly abundant bacterial hopanoids in Dajiuhu peatland, central China. Frontiers of Earth Science, 2009, 3, 320-326.	0.5	8

#	Article	IF	CITATIONS
145	Microbial influences on paleoenvironmental changes during the Permian-Triassic boundary crisis. Science China Earth Sciences, 2014, 57, 965-975.	5.2	8
146	Microbial roles equivalent to geological agents of high temperature and pressure in deep Earth. Science China Earth Sciences, 2016, 59, 2098-2104.	5.2	8
147	Volcanic ash stimulates growth of marine autotrophic and heterotrophic microorganisms. Geology, 0, , G38833.1.	4.4	8
148	Geobiological approach to evaluating marine carbonate source rocks of hydrocarbon. Science China Earth Sciences, 2011, 54, 1121-1135.	5.2	7
149	How Does Sphagnum Growing Affect Testate Amoeba Communities and Corresponding Protozoic Si Pools? Results from Field Analyses in SW China. Microbial Ecology, 2021, 82, 459-469.	2.8	7
150	Hydrocarbon compound evidence in marine successions of South China for frequent wildfires during the Permian-Triassic transition. Global and Planetary Change, 2021, 200, 103472.	3.5	7
151	Evolution of biotic carbon pumps in Earth history: Microbial roles as a carbon sink in oceans. Chinese Science Bulletin, 2022, 67, 1715-1726.	0.7	7
152	Wildfire response to rapid climate change during the Permian-Triassic biotic crisis. Global and Planetary Change, 2022, 215, 103872.	3.5	7
153	Geomicrobiological perspective on the pattern and causes of the 5-million-year Permo/Triassic biotic crisis. Frontiers of Earth Science, 2011, 5, 23-36.	2.1	6
154	Comparison of paleotemperature reconstructions using microbial tetraether thermometers of the Chinese loess-paleosol sequence for the past 350000 years. Science China Earth Sciences, 2017, 60, 1159-1170.	5.2	6
155	Comment on "Quantitative biochronology of the Permian–Triassic boundary in South China based on conodont unitary associations―by Brosse et al. (2016). Earth-Science Reviews, 2017, 164, 257-258.	9.1	6
156	Surface soil n-alkane molecular and ÎƊ distributions along a precipitation transect in northeastern China. Organic Geochemistry, 2020, 144, 104015.	1.8	6
157	Holocene forcing of East Asian hydroclimate recorded in a subtropical peatland from southeastern China. Climate Dynamics, 2023, 60, 981-993.	3.8	6
158	Recent achievements on the research of the Paleozoic-Mesozoic transitional period in South China. Frontiers of Earth Science, 2007, 1, 129-141.	0.5	5
159	Microbial Characteristics and Vegetation Changes as Recorded in Lipid Biomarker of Tianmushan Peat Bog. Earth Science Frontiers, 2008, 15, 170-177.	0.6	5
160	Absence of Middle Permian Kamura event in the Paleo-Tethys Ocean. Journal of Earth Science (Wuhan,) Tj ETQq0	0.0.rgBT / 3.2	Oyerlock 10
161	Moss-dwelling testate amoebae and their community in Dajiuhu peatland of Shennongjia Mountains, China. Journal of Freshwater Ecology, 2011, 26, 3-9.	1.2	5

¹⁶²Speleothem biomarker evidence for a negative terrestrial feedback on climate during Holocene warm
periods. Earth and Planetary Science Letters, 2019, 525, 115754.4.45

#	Article	IF	CITATIONS
163	Leaf Wax and Srâ€Nd Isotope Evidence for High‣atitude Dust Input to the Central South China Sea and Its Implication for Fertilization. Geophysical Research Letters, 2021, 48, e2020GL091853.	4.0	5
164	Influence of extraction methods on the distribution pattern and concentration of fatty acids and hydroxy fatty acids in soil samples: Acid digestion versus saponification. Geochemical Journal, 2016, 50, 439-443.	1.0	5
165	A â^¼60-Ma-long, high-resolution record of Ediacaran paleotemperature. Science Bulletin, 2022, 67, 910-913.	9.0	5
166	Lipid distribution in a subtropical southern China stalagmite as a record of soil ecosystem response to paleoclimate change. Quaternary Research, 2003, 60, 340-340.	1.7	4
167	How severe is the modern biotic crisis?—A comparison of global change and biotic crisis between Permian-Triassic transition and modern times. Frontiers of Earth Science, 2011, 5, 1-13.	2.1	4
168	Mechanisms of carbon storage and the coupled carbon, nitrogen and sulfur cycles in regional seas in response to global change. Science China Earth Sciences, 2017, 60, 1010-1014.	5.2	4
169	The shift of biogeochemical cycles indicative of the progressive marine ecosystem collapse across the Permian-Triassic boundary: An analog to modern oceans. Science China Earth Sciences, 2018, 61, 1379-1383.	5.2	4
170	Assessing the applicability of the long-chain diol (LDI) temperature proxy in the high-temperature South China Sea. Organic Geochemistry, 2020, 144, 104017.	1.8	4
171	Appraisal of paleoclimate indices based on bacterial 3-hydroxy fatty acids in 20 Chinese alkaline lakes. Organic Geochemistry, 2021, 160, 104277.	1.8	4
172	Contrasting distributions of bacterial branched tetraethers along a soil-river-lake transect in the arid region of Northwestern China. Geochemical Journal, 2016, 50, 249-265.	1.0	4
173	Episodic massive release of methane during the mid-Cretaceous greenhouse. Bulletin of the Geological Society of America, 2022, 134, 2958-2970.	3.3	4
174	Paleofire indicated by triterpenes and charcoal in a culture bed in eastern Kunlun Mountain, Northwest China. Frontiers of Earth Science, 2009, 3, 452-456.	0.5	3
175	Morphological variation and habitat selection of testate amoebae in Dajiuhu peatland, Central China. Journal of Earth Science (Wuhan, China), 2010, 21, 253-256.	3.2	3
176	Defining the discipline of geobiology. National Science Review, 2014, 1, 483-485.	9.5	3
177	The occurrence of a grassy vegetation over the Chinese Loess Plateau since the last interglacier: the molecular fossil record. Science in China Series D: Earth Sciences, 2002, 45, 53.	0.9	3
178	Bio-Organic Geochemistry research in China: Advances, opportunities and challenges. Science China Earth Sciences, 2018, 61, 1775-1780.	5.2	2
179	Peatland degradation in Asia threatens the biodiversity of testate amoebae (Protozoa) with consequences for protozoic silicon cycling. Geoderma, 2022, 420, 115870.	5.1	2
180	Distributions of phospholipid and glycolipid fatty acids in two strains of different functional Erythrobacter sp. isolated from South China Sea. Frontiers of Earth Science, 2009, 3, 91-99.	0.5	1

#	Article	IF	CITATIONS
181	Simulation experiments on the variation of leaf n-alkanes in aquatic environments. Frontiers of Earth Science, 2009, 3, 231-236.	0.5	1
182	Tectonomicrobiology: A new paradigm for geobiological research. Science China Earth Sciences, 2018, 61, 494-498.	5.2	1
183	Editorial: Refining the Interpretation of Nitrogen Isotopes in Deep Time Systems. Frontiers in Earth Science, 0, 10, .	1.8	1
184	An attempt to apply geobiological method in the source rock evaluation. Journal of Earth Science (Wuhan, China), 2010, 21, 312-314.	3.2	0